8-2019

Peroxide Sensing Using Nitrogen-Doped and Platinum Nanoparticle-modified Screen-Printed Carbon Electrodes

Chidiebere Ogbu
East Tennessee State University

Peroxide Sensing Using Nitrogen-Doped and Platinum Nanoparticle-modified Screen-Printed Carbon Electrodes

---

A thesis

presented to

the faculty of the Department of Chemistry

East Tennessee State University

In partial fulfillment

of the requirements for the degree

Master of Science in Chemistry

---

by

Chidiebere Ogbu

August 2019

Dr. Gregory Bishop, Chair

Dr. Dane W. Scott

Dr. Catherine McCusker

Keywords: Screen-Printed electrodes, nitrogen doping, hydrogen peroxide, platinum nanoparticles

ABSTRACT

Peroxide Sensing Using Nitrogen-Doped and Platinum Nanoparticle-modified Screen-Printed Carbon Electrodes

by

Chidiebere Ogbu

Nitrogen-doped carbon materials have garnered much interest due to their abilities to behave as electrocatalysts for reactions important in energy production (oxygen reduction) and biosensing (hydrogen peroxide reduction). Here, we demonstrate fabrication methods and determine electrocatalytic properties of nitrogen-doped screen-printed carbon (N-SPCE) electrodes. Nitrogen doping of graphite was achieved through a simple soft-nitriding technique which was then used in lab-formulated screen-printing inks to prepare N-SPCEs. N-SPCEs displayed good electrocatalytic activity, reproducibility and long-term stability towards the electrochemical reduction of hydrogen peroxide. N-SPCEs exhibited a wide linear range (20 µM to 5.3 mM), reasonable limit of detection of 2.5 µM, with an applied potential of -0.4 V (vs. Ag/AgCl). We also demonstrate that nitrided-graphite can similarly be used as a platform for the deposition of electrocatalytic platinum nanoparticles, resulting in Pt-N-SPCEs with a lower limit of detection (0.4 µM) and better sensitivity (0.52 µA cm^{-2} μM^{-1}) towards H_2O_2 reduction.

DEDICATION

This work is dedicated to my mother, Dr. Catherine Uchendu-Ogbu and my siblings.

ACKNOWLEDGMENTS

I am very grateful to my research advisor Dr. Gregory W. Bishop for his support, encouragement and guidance during this research work. I also want to appreciate Dr. Dane Scott and Dr. Catherine McCusker for their support and accepting to be on my thesis committee. I want to appreciate the faculty and staff of the Chemistry department for their assistance during my study at ETSU.

I am thankful to my mum, Dr. Catherine Uchendu-Ogbu, Dominic Igwe and my siblings, Emeka, Chinyere and Chidera, for their sacrifices and love. I want to thank my ever loving Meron Abbay, who has always encouraged me. My appreciation also goes to my colleagues in Dr. Bishop's research lab.

Acknowledgment is made to the Donors of the American Chemical Society Petroleum Research Fund for partial support of this research (XPS studies) through PRF# 58123-UNI5. Financial support of sensing studies was provided by the East Tennessee Foundation Butterfly Fund (grant number 23020). I also acknowledge ETSU Research and Sponsored Programs Administration (ETSU-ORSPA) for additional funding for this work. XPS was performed by Dr. Xu Feng at the Surface Analysis Laboratory in Department of Chemistry at Virginia Polytechnic Institute and State University, which is supported by the National Science Foundation under Grant No. CHE-1531834.

TABLE OF CONTENTS

LIST OF TABLES

Table Page

LIST OF FIGURES

Figure Page

LIST OF ABBREVIATIONS

Ag/AgCl	Silver/Silver Chloride reference electrode
CV	Cyclic Voltammetry
CNF	Carbon Nanofiber
DCC	Dicyclohexycarbodiimide
$FcCH_2OH$	Ferrocenemethanol
GCE	Glassy Carbon Electrode
GOx	Glucose Oxidase
HMT	Hexamethylenetetramine
LOD	Limit of Detection
MEA	β-mercaptoethylamine
MWCNTs	Multiwalled carbon nanotubes
$N\text{-}CNF_p$	Plasma Nitrided Electrospun Carbon Nanofiber
$N\text{-}CNF_{Th}$	Hydrothermal Nitrided Electrospun Carbon Nanofiber
N-GrNRs	Nitrogen doped graphene nanoribbons
N-SPCE	Nitrogen Doped Screen Printed Carbon Electrode
N-SEGN	Nitrogen-doped SonoElectrochemically produced Graphene Nanosheets
PtNPs	Platinum Nanoparticles
Pt-NSPCE	Platinum Modified Nitrogen Doped Screen Printed Carbon Electrode
PB	Prussian Blue
SPE	Screen Printed Electrodes
SPGFE	Screen-Printed Gold NanoFilm Electrode
RF	Radio Frequency
rGO	reduced Graphene Oxide

UNMNs	Ultrasmall Noble Metal Nanocatalysts
XPS	X-Ray Photoelectron Spectroscopy

CHAPTER 1

INTRODUCTION

Screen-printing technology offers high-volume production of reproducible, versatile, disposable and low-cost electrodes, which have found wide-spread use as sensors for electrochemical detection of various analytes.[1] Screen-Printed Electrodes (SPEs) are fabricated by printing a conductive ink or paste onto a plastic or ceramic substrate.[1] Inks are mixtures of conductive (e.g., metal or carbon) particles, polymeric binder, and solvent.[2] The use of inexpensive carbon sources instead of metals in conductive inks helps reduce cost. The binder serves as an adhesive to hold the conductive particles together. The solvent is used to dissolve the binder, and it also determines the viscosity of the ink as well as the curing and drying parameters.[3] Conductive screen-printing inks and pastes are commercially available or can be produced in-house.[4]

Since the 1990s, SPEs[4] have been used as sensing platforms in various applications ranging from biomedical,[5] pharmaceutical,[6] and environmental analysis.[7,8] Research on glucose sensors accounts for about 85 percent of the biosensor industry.[9] The most common and commercially significant use of SPEs is in the form of test strips for glucose meters, which are widely used by diabetics. The test strip is a glucose biosensor, which consists of a SPE (or other printed electrode) modified with glucose oxidase (GOx). The enzymatic reaction between glucose and GOx generates hydrogen peroxide (H_2O_2) which is oxidized at the SPE when held at a sufficient potential, resulting in an electrochemical signal in the form of a current that is proportional to the amount of glucose present.[9,10] Apart from its role in glucose sensing, hydrogen peroxide is also an important analyte in its own right due to its involvement in food processing, and in disease such as cancers.[10,11]

Hydrogen Peroxide Sensors Based on Screen-Printed Electrodes (SPEs)

Detection of hydrogen peroxide can be accomplished through direct oxidation ($H_2O_2 \rightleftharpoons O_2 + 2\ H^+ + 2\ e^-$) or reduction ($H_2O_2 + 2\ H^+ + 2e^- \rightleftharpoons 2\ H_2O$) on bulk electrodes. However, these processes are usually limited by slow electron transfer kinetics and high overpotentials (potential difference between the thermodynamically determined half-reaction and the potential at which the redox reaction is experimentally observed). Large overpotentials degrade sensing performance and lead to interference from other electroactive species such as ascorbate and urate when analyzing real samples.[11]

Overpotentials can be decreased and electron transfer kinetics can be improved for electrochemical reactions of H_2O_2 by applying various materials like hexacyanoferrates,[12,13] redox proteins,[14] and metal nanomaterials,[15,16] to electrodes or through oxygen plasma treatment[17] or doping the electrode surface with heteroatoms.[18,19,20]

Prussian Blue-Modified SPEs for H_2O_2 Sensing

Ferric hexacyanoferrate or Prussian blue (PB) is one material that has been shown to be electrocatalytic towards H_2O_2. In its reduced form (Prussian white), it can catalyze the reduction of H_2O_2 at low potentials.[13] Also, its polycrystalline structure confers excellent specificity for H_2O_2 reduction as it prohibits electron transfer with larger molecules like uric acid and ascorbic acid.[21] Ricci et al. modified graphite powder with *in situ* chemically synthesized PB to fabricate SPEs.[22] The PB-modified SPE showed a linear range of 0.1-50 µM with a limit of detection (LOD) of 0.1 µM and a sensitivity of 324 µA mM^{-1} cm^{-2} for H_2O_2 reduction. Other groups have also developed PB-based sensors with nanomaterials to improve sensitivity and limit of detections towards H_2O_2 detection.[23,24] The major downside to using PB is that its reduced form can be dissolved by hydroxide ions. This impacts the stability of PB in neutral or alkaline

solutions.[13] However, recent studies have demonstrated that surfactants can enhance the electrochemical stability of PB in basic solutions.[11]

Plasma Treatment of SPEs for Oxidation of H_2O_2

Oxygen plasma treatment is another strategy that has been employed to improve the electrochemical properties of SPEs.[25] Wang et al. developed a strategy that involved using a radio frequency (RF) O_2 plasma to remove binder and other impurities from the surface of carbon SPEs. The process was also found to increase defects on graphite particles that define the electrode surface, thereby improving the kinetics of electrochemical reactions on the electrode. O_2 plasma treatment improved the sensitivity of commercially available SPEs towards H_2O_2 oxidation by about 80-fold compared to SPEs used without prior plasma treatment.[17]

Metal Nanoparticle-Modified SPEs for H_2O_2 Sensing

Transition metal nanomaterials have also been widely used for enhancing SPE sensitivity for detection of H_2O_2.[26-28] Earlier studies by Chikae et al. reported a strategy for the detection of H_2O_2 using platinum nanoparticles (PtNPs) deposited on SPEs via electrodeposition. The SPE was covered with 30 µL of 1 mM $PtCl_2$ prepared in 0.1 M HCl (pH 1.2), and a potential of -0.4 V (vs. Ag/AgCl) was applied to the electrode for 1-200 seconds to deposit PtNPs. The modified SPEs showed improved electrocatalytic activity towards H_2O_2 oxidation with a linear range of 16 µM to 2 mM and a detection limit of 16 µM.[29]

Niu and coworkers[30] reported an H_2O_2 sensor based on platinum nanoparticles decorated carbon nanotubes clusters on screen-printed gold nanofilm electrode (SPGFE). Multiwalled carbon nanotubes (MWCNTs) were first carboxy functionalized by mixing with H_2SO_4 (3:1 v/v) and HNO_3. The mixture was sonicated for 4 hrs, rinsed and dried at a temperature of 50 °C. Dicyclohexycarbodiimide was mixed with treated MWCNTs dispersed in water. The SPGFE

substrate was incubated in a solution containing β-mercaptoethylamine (MEA) for 6 hrs to obtain an oriented MEA monolayer. The MEA-modified electrode was incubated in the carbon nanotube solution for 8 hrs. PtNPs were electrodeposited on the MWCNT structure by applying a potential from +0.3V to +1.3V to a solution containing chloroplatinic acid (H_2PtCl_6) followed a potential of -0.3V to +1.0V in 0.5 M H_2SO_4 to a steady state. The modified SPGFE showed improved electrocatalytic activity towards H_2O_2 reduction with a LOD of 1.23 μM and linear range of 0.05 mM to 2 mM. In recent studies, very low detection limits of about 0.04 μM[31] and 0.2 μM[32] have been reported using platinum nanoparticles.

Metal Nanoparticle Size and Electrocatalytic Activity

Various studies have shown that catalytic activities of metal nanoparticles are size dependent with ultrasmall metal nanocatalyst (<2 nm) attracting considerable attention.[33] Wide variations in particle sizes occur when impregnation or coprecipitation are used to deposit metal nanoparticles on supports (e.g., carbon). Variations in particle sizes have been attributed to weak affinity of the metal precursors or their nanocatalysts to the support.[34] Various groups have tried to solve this problem by using capping agents to control the sizes and nanostructures, and to prevent overgrowth.[35] However, this method causes the blockage of catalytic sites leading to decreased activity and selectivity. The removal of the capping agents through oxidation and thermal decomposition can lead to sintering of the nanoparticle thereby causing loss of surface-active sites.[34]

"Soft" Nitriding for Deposition of Metal Nanoparticles on Carbon

Liu et al. recently reported a strategy for "soft-nitriding" of carbon that enables deposition of highly catalytically active metal nanoparticles on carbon black, activated carbon, and

mesoporous carbon supports. This process involves annealing a carbon source with urea at a temperature of 300°C to introduce surface nitrogen groups onto which ligand-free ultra-small (<2 nm) noble metal particles can be preferentially deposited via chemical reduction of metal precursors (e.g. $HAuCl_4$, K_2PdCl_6 or K_2PtCl_6) using $NaBH_4$ as a reducing agent. The small-sized, ligand-free metal nanoparticles exhibited greater electrocatalytic activities towards methanol oxidation compared to others with surface capping agents.[33]

N-doped Carbon Electrodes for H_2O_2 Sensing

Aside from using nitrogen doping to deposit electrocatalytically active metals onto carbon, other studies have found that nitrogen-doped carbon can itself act electrocatalytically towards H_2O_2 reduction.[36,37,38] Liu et al. synthesized nitrogen-doped carbon that exhibited good electrocatalytic activity towards the reduction of H_2O_2.[39] Hexamethylenetetramine (HMT) was used as both a carbon and nitrogen source because it possesses high nitrogen content. N-carbon was synthesized by heat treatment of HMT for 30 min in air at a temperature of 300 ^oC. XPS analysis showed that 27.86 wt% of nitrogen atoms were incorporated onto the carbon surface. The N-carbon was used to modify a glassy carbon electrode (GCE) by a simple drop-casting method. The N-carbon modified GCE was used as an amperometric sensor for H_2O_2. Using an applied potential of -0.3 V, the sensor exhibited a limit of detection of 90 µM and a linear range of 0.1-40 mM. Another group reported ultrathin graphitic carbon nitride nanosheets sensors, which were fabricated by ultrasonication-assisted liquid exfoliation of the bulk material (g-C_3N_4). The nitrogen-doped carbon electrodes were electrocatalytic towards H_2O_2 reduction with a LOD of 2.0 µM and a linear range of 0.1-90 mM.[40] Lyu et al. compared electrocatalytic activities of hydrothermal (N-CNF_{Th}) and plasma nitrided electrospun carbon nanofiber (N-CNF_p) modified GCEs towards the reduction of H_2O_2. Electrospun polymer fibers were

converted to carbon nanofibers (CNF) by high temperature treatment under argon at a temperature of 1300 ^{o}C. For N-CNF$_p$ preparation, briefly, the CNF were treated with nitrogen plasma at a power of 100 W and a flow rate of 40 cm^3 min^{-1}. For N-CNF$_{Th}$, the CNF was ground into powdered form and mixed with aqueous urea solution using ultrasonic vibration. The obtained solution was hydrothermally reacted in an autoclave at a temperature of 180 ^{o}C for 12 hrs. XPS data showed nitrogen wt% of 3% and 7% for the N-CNF$_{Th}$ and N-CNF$_p$, respectively. They concluded that N-CNF$_{Th}$ with its rough surface and complex profiles of doped nitrogen, was more catalytically active with a LOD of 0.62 µM compared to the N-CNF$_p$ with a LOD of 1.84 µM.[20]

Another strategy reported for N-doping of carbon involves mixing graphene nanoribbons (GrNRs) with aqueous ammonia at a temperature of 80 ^{o}C for 6 hrs. The N-GrNRs was then dispersed in water via ultrasonication, and the suspension was drop-casted on the working electrode SPE, followed by drying in air. An atomic surface nitrogen content of 16.18 wt% was observed from the XPS analysis of N-GrNRs. N-GrNR-modified SPEs were found to be electrocatalytic towards reduction of H_2O_2 with a LOD of 1.72 µM and a linear range of 0.005-2.8 mM.[18]

Wu and coworkers[41] studied the effect material structures can have on the electrocatalytic activity towards H_2O_2 using another nitrogen doping method. They compared nitrogen-doped sonoelectrochemically produced graphene nanosheets (N-SEGN) with nitrogen-doped reduced graphene oxide (N-rGO).[42] SEGN and rGO were nitrided separately using the same method by reacting graphene nanosheets or reduced graphene oxide with tetra-2-pyridinyl pyrazine in an autoclave. The N-SEGN and N-rGO were then drop-casted on separate GCEs. XPS analysis of the N-SEGN and N-rGO showed a nitrogen content of 2.6% and 3.7% respectively. They

concluded that N-SEGN was more electrocatalytic towards H_2O_2 sensing with an LOD of 0.8796 μM, a sensitivity of 231.3 μA $mM^{-1}cm^{-2}$ and a linear range of 0.01-2.225 mM compared to N-rGO with an LOD of 0.9946 μM, sensitivity of 57.3 μA $mM^{-1}cm^{-2}$ and a linear range of 0.01-4.625 mM. They attributed the better performance of the N-SEGN to its vacancies in the structure that enabled an increased amount of pyrollic nitrogen to be deposited which may enhance charge mobility and donor acceptor property, important factors in H_2O_2 sensing.

Research Objectives

Although different strategies have been reported using N-doped carbon for H_2O_2 sensing, most involve modifications of the electrode surface and complex preparation processes, thus requiring additional steps before use. We demonstrate a simple, low-cost and direct method for fabricating nitrogen-doped screen-printed electrodes (N-SPCEs). This method eliminates the need for modification of the electrode after printing the electrodes. Nitrogen doping of the carbon was achieved through a simple "soft" nitriding technique using urea[33], which was then used in formulating a conductive ink. SPCEs were then fabricated using the ink. The electrocatalytic activity of N-SPCEs towards the reduction of H_2O_2 was investigated through cyclic voltammetry. Amperometric sensors for H_2O_2 based on N-SPCE platforms exhibited wide linear range, favorable detection limit, and good stability and reproducibility[33]

Nitriding of carbon not only increases its electrocatalytic activity towards H_2O_2, but it also enables deposition of highly catalytically active metal nanoparticles on carbon surfaces.[33] In this work, we also demonstrate that nitrided-graphite can similarly be used as a platform for the deposition of electrocatalytic platinum nanoparticles and report their electrocatalytic activity towards H_2O_2 reduction.

CHAPTER 2

EXPERIMENTAL

Materials

All chemicals were used as purchased from the manufacturer. Potassium chloride, ferrocenemethanol, urea, cellulose acetate, bovine calf serum and graphite powder were purchased from Sigma Aldrich. H_2O_2 (30 wt%), NaCl, KCl, Na_2HPO_4 and KH_2PO_4, K_2PtCl_4 were purchased from Acros Organics. Ethyl alcohol was procured from Pharmco Products Inc. All aqueous solutions were prepared with 18.2 MΩ·cm ultrapure water, obtained by passing water through a Millipore Synergy purifier. Phosphate buffered saline solution (pH= 7.4) was prepared by mixing 8 g of NaCl, 0.2 g of KCl, 1.44 g of Na_2HPO_4, 0.24 g of KH_2PO_4, in 800 mL of distilled water. The pH was adjusted using NaOH or HCl and diluted to 1 L. The pH of 7.4 was used because of the potential application of the sensor for measurement of biological samples.

Nitrogen Doping of Graphite Powder

Nitrogen doping of graphite was achieved through a previously reported "soft" nitriding protocol[33] with some modification. Graphite powder (1 g) was mixed with solid urea (1.5 g) using mortar and pestle. The mixture was annealed at 150 ^oC for two hours using a temperature-controlled oven, followed by further heating at 250 ^oC for two hours. The product was washed with 20 mL of water followed by 20 mL of ethanol and the process repeated 3 times. The resulting N-doped graphite was put in a crucible after washing then dried at 70 ^oC for 30 mins in a temperature-controlled oven, then dried in air overnight before use.

In Situ Growth of PtNPs on Nitrided Graphite Powder

PtNPs were grown on the nitrogen-doped graphite powder *in situ* through a previously described method[33] using K_2PtCl_4 as the metal source and $NaBH_4$ as the reducing agent. Nitrogen doped graphite (1 g) was added to 2 L of water and sonicated for 30 min. 50 mg of K_2PtCl_4 was added and stirred for an additional 2 hrs. 60 mL of ice-cooled and freshly prepared $NaBH_4$ solution (1 mg/mL) was quickly injected into the above solution. The solution was stirred for 2 hrs and washed with water and ethanol to remove unreacted K_2PtCl_4. The Pt-N graphite was dried and used in formulating a conductive ink which was then used for Pt-NSPCE fabrication.

X-ray Photoelectron Spectroscopy (XPS)

X-ray photoelectron spectroscopy analysis of carbon was carried out by Dr. Xu Feng at the Surface Analysis Laboratory at Virginia Tech. using a PHI VersaProbe III scanning XPS microscope. The system uses a monochromatic Al K-alpha X-ray source (1486.6 eV). The spectra were acquired with a 200 µm/50 W/15 kV X-ray settings and dual-beam charge neutralization. Binding energies were referenced to sp^2 carbon peak at 284.3 eV. Relative surface atomic concentration % of elements were determined from the integrated intensity of the elemental photoemission features corrected by relative atomic sensitivity factors.

Conductive Ink Formulation and SPCE Fabrication

Graphite, N-doped graphite and Pt-N-graphite were used to make three separate conductive inks to prepare SPCEs, N-SPCEs and Pt-N-SPCE for comparison studies. Cellulose acetate (0.06 g) (polymeric binder), cyclohexanone (1 mL), acetone (1 mL) were mixed by ball milling and sonicated for 20 mins to obtain a homogenous mixture.[43] Then, graphite, N-graphite powder or Pt-N-graphite powder (0.94 g) was added into the mixture and sonicated for 40 min,

resulting in a conductive ink. SPCE, N-SPCE and Pt-NSPCE working electrodes were manually printed using a 110-mesh screen prepared as previously described.[44] The geometric average surface areas for SPCE and N-SPCEs, Pt-NSPCE were measured to be 0.027 (±0.009) cm^2, 0.029 (± 0.003) cm^2 and 0.028 (±0.005) cm^2, respectively, using ImageJ software as previously described.[45] Briefly, the image of an electrode with a caliper close to it for scale was taken using a digital camera and exported to ImageJ software. A calibration scale was then set in the software using a known distance measured from the caliper. The boundary of the electrode was then traced in the software, and the software's measurement tool converted the electrode area from pixels to cm^2.

Electrochemical Measurements

All electrochemical measurements were obtained using a CH Instruments 1040C electrochemical analyzer with SPCE, N-SPCE or Pt-N-SPCE working electrode, Ag/AgCl (1 M KCl) as reference electrode, and a platinum wire counter electrode. Electrochemical data were recorded and are presented using the typical electrochemical convention with negative currents corresponding to oxidation processes and positive currents corresponding to reduction processes. All currents were converted to current density by normalizing using the geometric area of the individual electrodes employed for each experiment to compensate for variations in electrode sizes.

Cyclic Voltammetry

For characterization of SPCEs and N-SPCEs, 10 mL of solution containing 0.5 mM ferrocenemethanol ($FcCH_2OH$) (redox probe) was prepared in 0.1 M potassium chloride (KCl) supporting electrolyte. A SPCE or N-SPCE was placed in the solution along with reference and

counter electrodes, and cyclic voltammetric (CV) measurements were then carried out at a scan rate 50 mV s^{-1}.

To evaluate electrochemical behavior of H_2O_2 at SPCEs and modified SPCEs (N-SPCEs and Pt-N-SPCEs), 10 mL solution containing 0.05 M Phosphate buffer (pH 7.4) was poured in a beaker. CVs were taken for the different fabricated electrodes at a scan rate of 50 mV s^{-1}. Futhermore, 20 µL of stock solution (30 wt %) of H_2O_2 was added into the solution for a concentration of 20 mM, and the solution mixed. CVs were again taken for the electrodes at the same scan rate.

Amperometry

Electrodes were placed in a beaker containing 20 mL of 0.05 M phosphate buffer solution. The solution was stirred using a magnetic stirrer to enable fast attainment of steady-state current. The working electrode potential was held at -0.4 V vs. the Ag/AgCl reference. The current-time response was measured by adding 4 µL, 10 µL, 20 µL and increments of 20 µL up to 200 of a 100 mM H_2O_2 solution (102.2 µL of 30 wt% H_2O_2 stock solution in 10 mL phosphate buffer solution). These amounts were added successively into the stirred buffer solution every 50 seconds and the steady state current recorded after each addition to obtain a calibration curve.

Spiked Recovery of Bovine Calf Serum

Hydrogen peroxide (100 mM) was prepared in bovine calf serum by mixing 20.4 µL of 30 wt% H_2O_2 solution in 2 mL of bovine calf serum. Volumes (16, 80 and 500 µL) of the mixture were spiked in 20 mL of stirred phosphate buffer solution to obtain H_2O_2 concentrations of 0.08 mM, 0.4 mM and 2.5 mM.

CHAPTER 3

RESULTS AND DISCUSSION

Soft Nitriding of Graphite

X-Ray Photoelectron Spectroscopy (XPS) as surface analysis technique was used to determine the surface composition of the undoped and nitrogen doped graphite. XPS results demonstrate clear differences between unmodified graphite and graphite modified via soft nitriding with urea (Figure 1). Prior to soft nitriding, graphite exhibited only one strong C1s peak at 284.3 eV (Figure 2a), which is consistent with sp^2 carbon. After nitriding, 2 major C1s peaks are observed (Figure 2b). In addition to the sp^2 peak, there is a second major peak at 289.71 eV. Also, the sp^2 peak appears broader towards higher energies for nitrided graphite compared to unmodified graphite, which is likely the result of the introduction of functional groups like oxygen- and/or nitrogen-containing functional groups.[46]

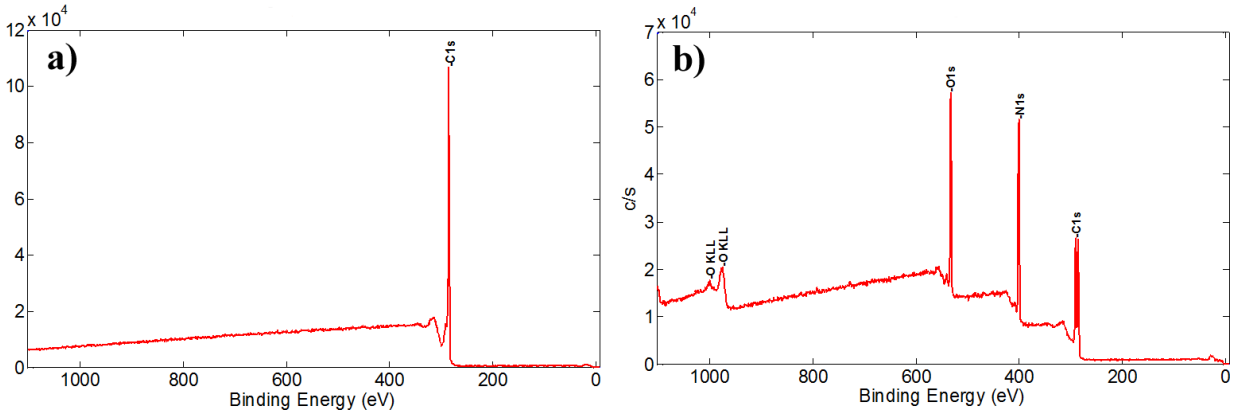

Figure 1. XPS spectra of graphite (a) and nitrogen-doped graphite (b).

In a previous study, Liu and coworkers similarly observed C1s peaks at ~284 eV and ~289 eV after nitriding Printex G, a carbon black with urea. They attributed the peaks to sp^2 carbon (284 eV) and sp^3 carbons with C-O and C-N bonds (289 eV). However, C1s peaks associated with C=O and C-N are known to overlap with binding energies of ~287 to 288 eV,[36]

making it difficult to confirm nitrogen doping based on the C1s peak at ~289 eV. The C1s peak at 289 eV in our studies and the previous work may alternatively suggest that unreacted urea or thermal decomposition products of urea are present on the carbon surface as the position of the peak is consistent with C1s for O=C-N compounds.[47] Schaber and coworkers[48] reported that heat treatment of urea at 250 °C results in nearly complete (~99%) thermal decomposition with cyanuric acid (produced from the reaction of decomposition products biuret and cyanic acid, HCNO) as the main product and smaller amounts of ammelide (cyanic acid + urea) and ammeline (ammelide + ammonia). All of these products of thermal decomposition contain O=C-N in their keto forms (Figure 3).

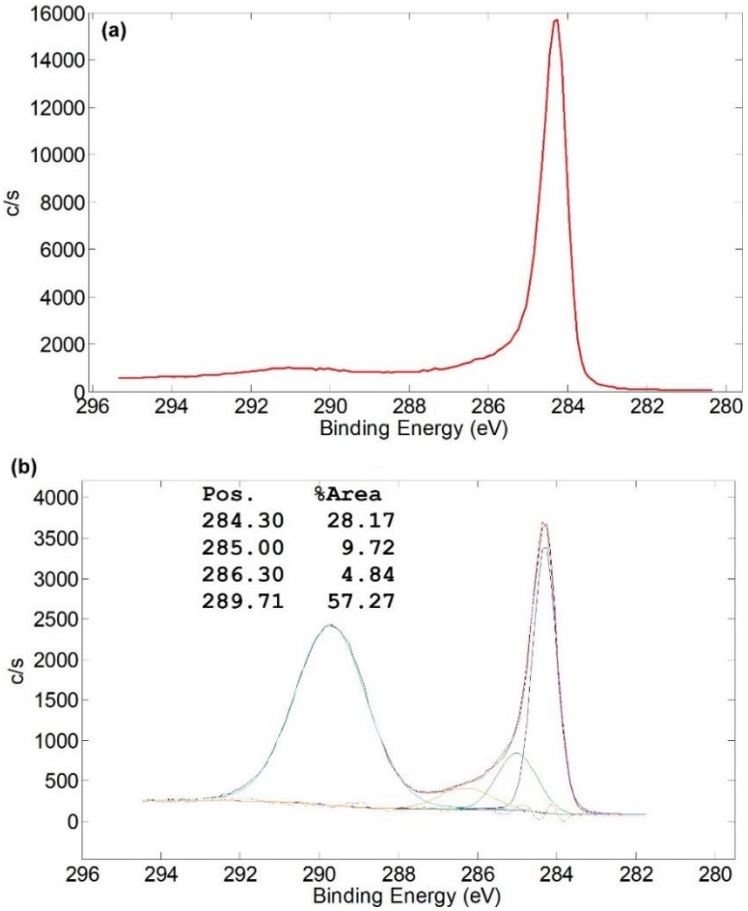

Figure 2. XPS spectra of C1s (a) graphite, and (b) nitrogen-doped graphite.

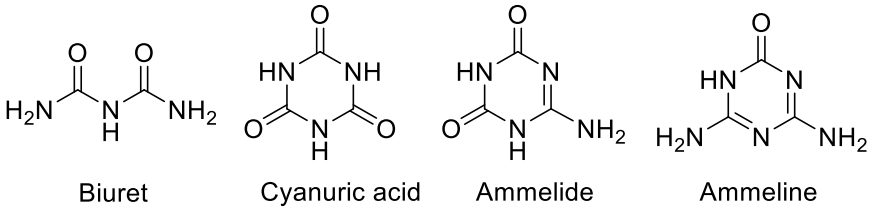

Figure 3. Products of thermal decomposition of urea.

While XPS of unmodified graphite produced no peak for nitrogen and only a very small peak for oxygen, N1s (400.69 eV) and O1s (532.20 eV) peaks were obvious on the nitrided graphite (Figure 1b). Relative surface atomic concentrations of nitrogen and oxygen from these peaks on N-doped graphite were 32.72% and 18.66%, respectively (Table 1). For comparison, Liu et al. estimated surface nitrogen content to be 19 atom % on soft-nitrided Printex G.[33]

Table 1. Relative surface atomic concentration % of C, N, and O for the undoped carbon and doped carbon.

Material	Carbon	Nitrogen	Oxygen
Graphite	99.77	0	0.23
N-Doped Graphite	48.62	32.72	18.66

The broad N1s peak can be deconvoluted (to determine the type of nitrogen species present in the nitrogen doped graphite) into 3 signals having binding energies of 399.39 eV which corresponds to pyridinic-N, 400.69 eV corresponds to amine/amide-N and 401.67 eV corresponding to quaternary-N (Figure 4). The surface atomic concentrations of the different types of nitrogen species showed that the majority of nitrogen atoms on the N-doped graphite (55%) were found to be amine/amide. In comparison, Liu and coworkers[33] observed that 68% of the nitrogen atoms introduced by nitriding Printex G, were amine/amide in nature, while lower

percentages of pyridinic (15%) and quaternary (17%) were also found. The presence of quaternary and pyridine N atoms in XPS was offered as evidence of nitriding into the graphitic layers. However, it should be noted that these N1s peaks can also come from urea and thermal decomposition products of urea (Figure 3).

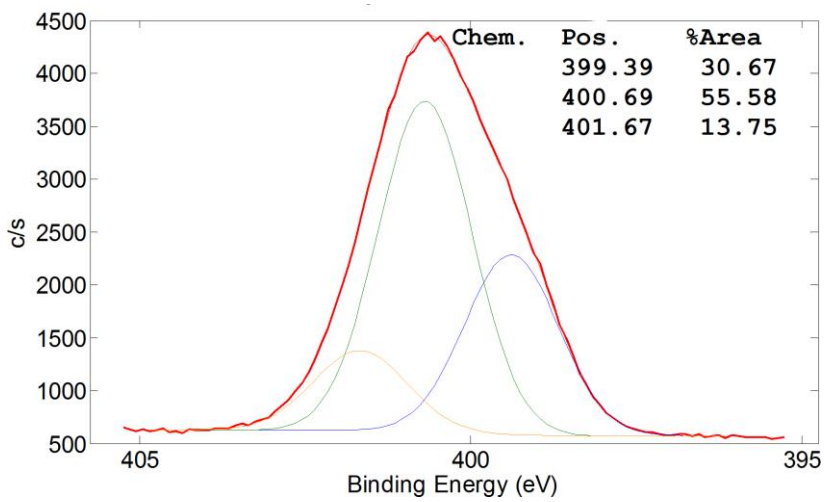

Figure 4. Deconvoluted XPS N1s peak of nitrogen-doped graphite. N1s peak (red) is composed of peaks at 399.39 (yellow, pyridinic N), 400.69 (green, amine/amide N), and 401.67 (blue, quaternary N).

Liu and coworkers[33] suggested that soft nitriding occurred mainly through chemical modification of oxygen containing sites on the surface of carbon black. However, from our results, since graphite contained minimum amount of oxygen, nitriding may have instead or additionally resulted in the intercalation of urea and/or its decomposition products between the graphite layers.

Electrochemical Characterization of SPCEs and N-SPCEs

SPCEs and N-SPCEs were characterized by CV using ferrocenemethanol ($FcCH_2OH$) as a redox probe. Voltammetric peak-to-peak separation of the oxidation and reduction peaks (ΔE_p) for a reversible one-electron redox reaction like that which corresponds to the

$FcCH_2OH/FcCH_2OH^+$ redox couple are expected to be 59 mV.[49] Peak-to-peak separations for the $FcCH_2OH/FcCH_2OH^+$ redox couple on SPCE and N-SPCE were 201 mV and 109 mV, respectively (Figure 5), which are comparable to those found for other commercially available SPCEs,[49,50] and indicate suitable behavior for electrochemical applications.

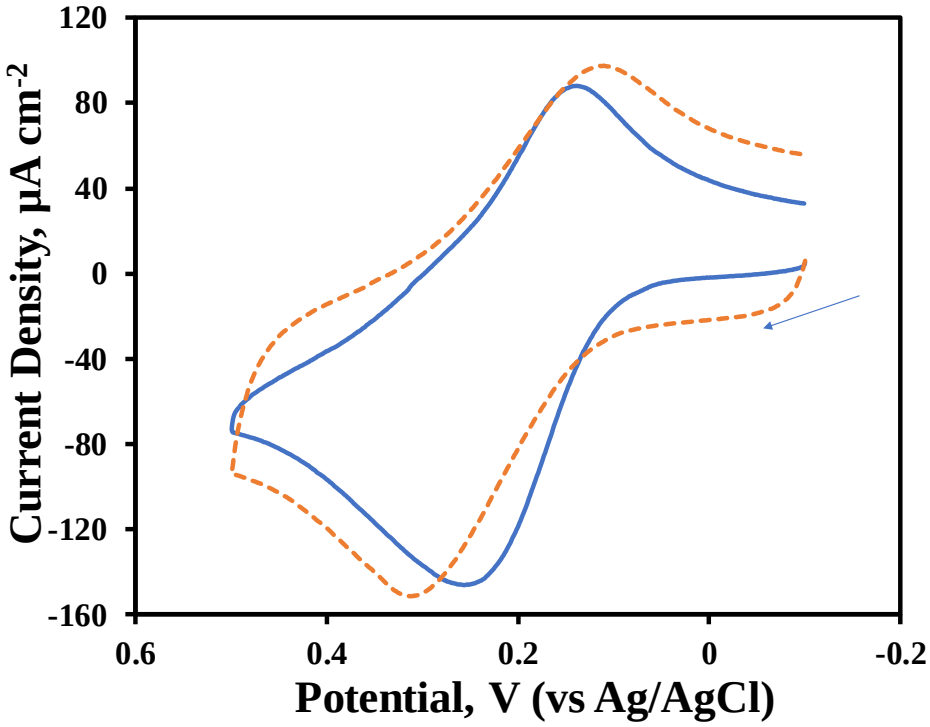

Figure 5. Representative CVs of 0.50 mM ferrocenemethanol in 0.10 M KCl with bare SPCE (orange dotted lines) and N-SPCE (blue lines). Arrow indicates direction of scan. Scan rate of 50 mVs^{-1}

Electrocatalytic Performance of N-SPCEs Towards Reduction of H_2O_2

Various studies[18,20,36] have shown that N-doped carbon materials can act electrocatalytically towards the reduction of H_2O_2. While CVs of both SPCEs and N-SPCEs show an onset potential of around +0.5 V for the oxidation of H_2O_2 in 0.05 M phosphate buffer (Figure 6), N-SPCEs exhibited significant electrocatalytic behavior toward H_2O_2 reduction compared to SPCEs. SPCEs showed only a slight increase in reduction current at potentials more

negative than -0.2 V after exposure to 20 mM H_2O_2 in 0.05 M phosphate buffer (pH 7.4) (Figure 6a). In contrast, a notable reduction response with an onset potential of -0.08 V and high cathodic current is observed for the N-SPCE (Figure 6b) when the electrode is exposed to same concentration of H_2O_2 under the same conditions. This suggests that the N-SPCE can effectively catalyze the electrochemical reduction of H_2O_2 at low potential, which is consistent with previously reported literature.[18,36,39]

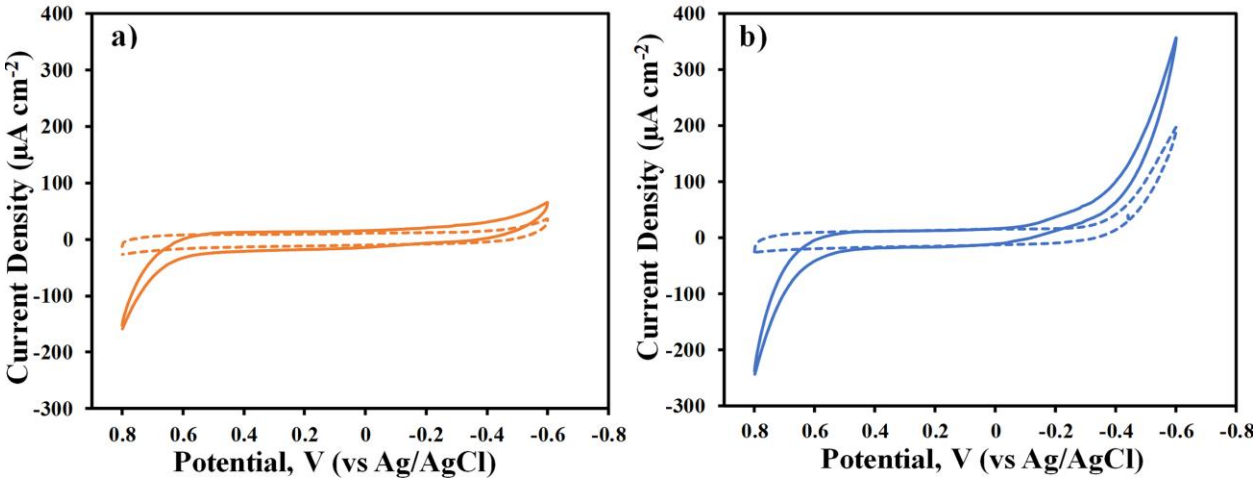

Figure 6. CV responses for SPCEs in the absence (dotted lines) and presence (solid lines) of 20 mM H_2O_2 for a) Bare-SPCE (orange line) and b) N-SPCE (blue line). All CVs were obtained in 0.05 M phosphate buffer (pH 7.4) at a scan rate of 50 mVs^{-1}.

The mechanism for electrochemical reduction of H_2O_2 can be summarized by the following steps:[18,51]

$$H_2O_2 + e^- \rightarrow OH_{ad} + OH^-$$

$$OH_{ad} + e^- \rightarrow OH^-$$

$$2OH^- + 2H^+ \rightarrow 2H_2O$$

As shown above, breaking the O-O bond is a crucial step in the electrocatalytic reduction of H_2O_2.[36] The electrocatalytic behavior of N-doped carbons has been attributed to free electrons of nitrogen atoms, which can facilitate breaking of the O-O bond.[51,18]

Amperometric responses of the SPCEs and N-SPCEs using an applied potential of -0.4 V were recorded in phosphate buffer while increasing concentrations of H_2O_2 were added to the solution by spiking every 50 seconds (Figure 7). When H_2O_2 was added into a stirred buffer solution, N-SPCE responded to the analyte with a characteristic step-wise response where the current increased rapidly to reach a stable value. The cathodic current increased with increasing concentration of H_2O_2 using the N-SPCE, (Figure 7a) while the SPCE displayed no change in current on successive addition of the same concentrations of H_2O_2.[18,52]

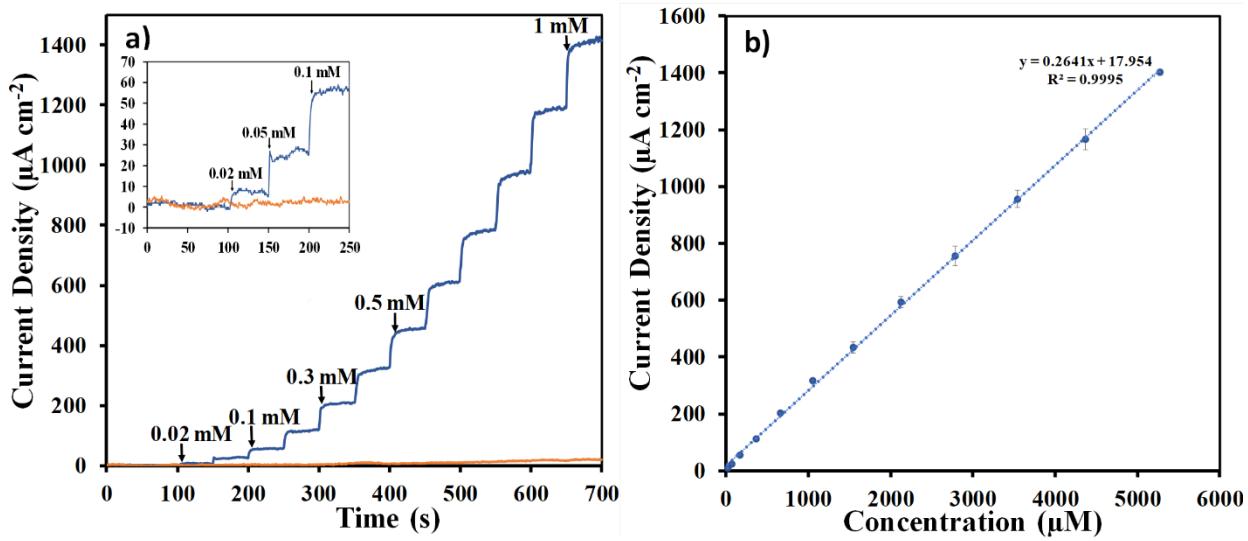

Figure 7. a) Amperometric responses of SPCE (orange) N-SPCE (blue) upon successive additions of H_2O_2 at different concentrations into 0.05M phosphate buffer (7.4) at -0.4 V. b) Calibration curves for detection of H_2O_2 via amperometry using N-SPCEs. Error bars correspond to one standard deviation of response of 4 different electrodes.

The analytical performance of the N-SPCEs compares favorably to other H_2O_2 sensors based on nitrogen-doped carbons (Table 2). Calibration plots (Figure 7b) indicate a good linear relationship (R^2=0.9995) between measured current density and H_2O_2 concentration over the range of 20 µM to 5.3 mM. The sensitivity of N-SPCEs towards hydrogen peroxide sensing was 0.264 (± 0.005) µA cm^{-2} $µM^{-1}$ and the limit of detection was calculated to be 2.5 µM using three

times the standard deviation of the background signal, divided by the sensitivity of the N-SPCE For comparison, Shi et al.[18] reported a limit of detection of 1.72 μM, linear ranges of 0.005-0.085 mM and 0.135-1.285 mM, and sensitivities of 2.18 μA cm^{-2} μM^{-1} and 0.64 μA cm^{-2} μM^{-1} for the two different linear ranges using nitrogen doped graphene nanoribbons for amperometric detection of H_2O_2 at -0.4 V.

Table 2. Comparison of analytical performance of some N-doped amperometric H_2O_2 sensors.

Materials	**Potential (V)**	**Linear range (mM)**	**Sensitivity (μA cm^{-2} μM^{-1})**	**LOD (μM)**	**Ref.**
N-Graphene Nanoribbons	-0.4	0.005-0.085, 0.135-1.285	2.18, 0.64	1.72	18
Carbon nitride nanosheet	-0.3	0.1-90	-	2.0	40
N-doped Carbon	-0.3	0.1-40	-	90	39
$N\text{-}CNF_{Th}$	-0.4	0.01-0.71, 0.71-2.91	0.357, 0.203	0.62	20
$N\text{-}CNF_{p}$	-0.4	0.01-0.21, 0.21-2.21	0.257, 0.180	1.84	20
Mesoporous carbon nitride	-0.19	0.004-0.04, 0.04-12.4	0.642	1.52	53
N-SPCE	-0.4	0.02-5.3	0.264	2.5	This work

In addition to linear range, LOD, and sensitivity, reproducibility and stability are also important properties that must be considered when assessing the analytical performance of electrochemical sensors. Average signals for four different N-SPCEs differed by no more than % upon exposure to H_2O_2 at concentrations ranging from 20 μM to 5.3 mM, indicating good reproducibility of the sensors. Stability of the sensors was monitored by repeating measurements

of 1 mM H_2O_2 over a period of 14 days. The sensor was stored at room temperature in between measurements. Response dropped by only ~2% after 2 days, and the sensor retained 92% of its response after one week and 89% after 2 weeks, signifying that the sensor showed good long-term stability (Figure 8) at a level that is comparable with other reported works.[18,40]

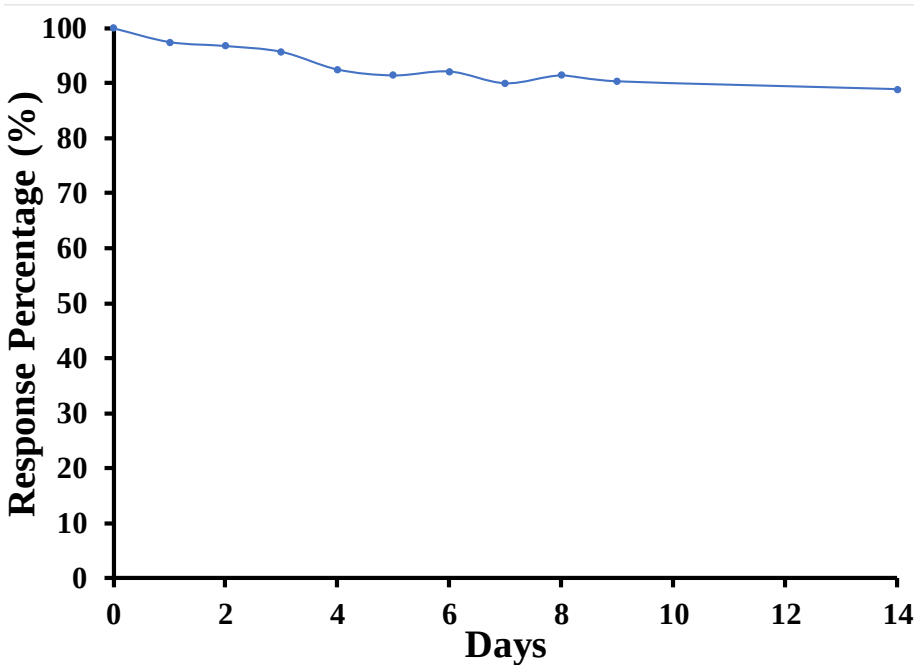

Figure 8. The variation in the response current of N-SPCE for 14 days.

The feasibility of N-SPCE to be used as sensors for real samples was evaluated using bovine calf serum as a complex matrix, since bovine calf serum was previously shown to be a good surrogate for human serum in the development of electrochemical biosensors.[54,55] Spike recoveries of the known H_2O_2 concentrations (0.08 mM, 0.4 mM and 2.5 mM) were determined based on the amperometric signals and related to the equation of the calibration curve (Figure 7b). Average spike recoveries ranged from 93.0 to 99.5% with RSDs of 6.6% or less based on three measurements, indicating that N-SPCEs are applicable for H_2O_2 detection in complex samples. (Table 3)

Table 3. Detection of H_2O_2 in Bovine Calf Serum using N-SPCEs.

Add (mM)	Found (mM)	RSD	Recovery (%)
0.08	0.074	2.89	93.0
0.40	0.393	6.64	97.6
2.50	2.487	2.53	99.5

Performance of Pt-N-SPCE for H_2O_2 Sensing

Although N-SPCEs were electrocatalytic towards H_2O_2 reduction, the limit of detection and sensitivity can be improved by incorporating metal nanoparticles on the electrode surface. Liu and coworkers[33] reported that nitriding enables ligand-free ultrasmall (< 2nm) noble metal nanocatalysts to be deposited onto carbon. We fabricated Pt-N-SPCEs (see experimental section) and compared their electrocatalytic activity towards hydrogen peroxide reduction to N-SPCEs.

A notable reduction response with an onset potential of -0.031 V and a high cathodic current are observed for Pt-N-SPCE after exposure to 20 mM H_2O_2 in 0.05 M phosphate buffer (Figure 9), compared to the N-SPCE which has an onset reduction potential of -0.08 V and a lower cathodic current for the same concentration of H_2O_2 under the same conditions (Figure 6b)

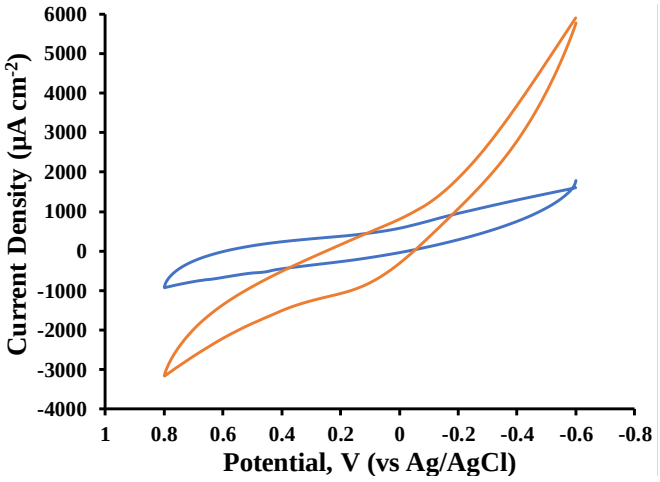

Figure 9. CV responses for Pt-N-SPCEs in the absence (blue lines) and presence (orange lines) of 20 mM H_2O_2. All CVs were obtained in 0.05 M phosphate buffer (pH 7.4) at a scan rate of 50 mVs^{-1}.

Amperometric responses of the Pt-N-SPCEs using an applied potential of -0.4 V were recorded in phosphate buffer while increasing concentrations of H_2O_2 were added to the solution by spiking. When H_2O_2 was added into a stirred buffer solution, Pt-N-SPCE responded to the analyte with a characteristic step-wise response where the current increased rapidly to reach a stable value. The cathodic current increased with increasing concentration of H_2O_2 using the Pt-N-SPCE, (Figure 10a).

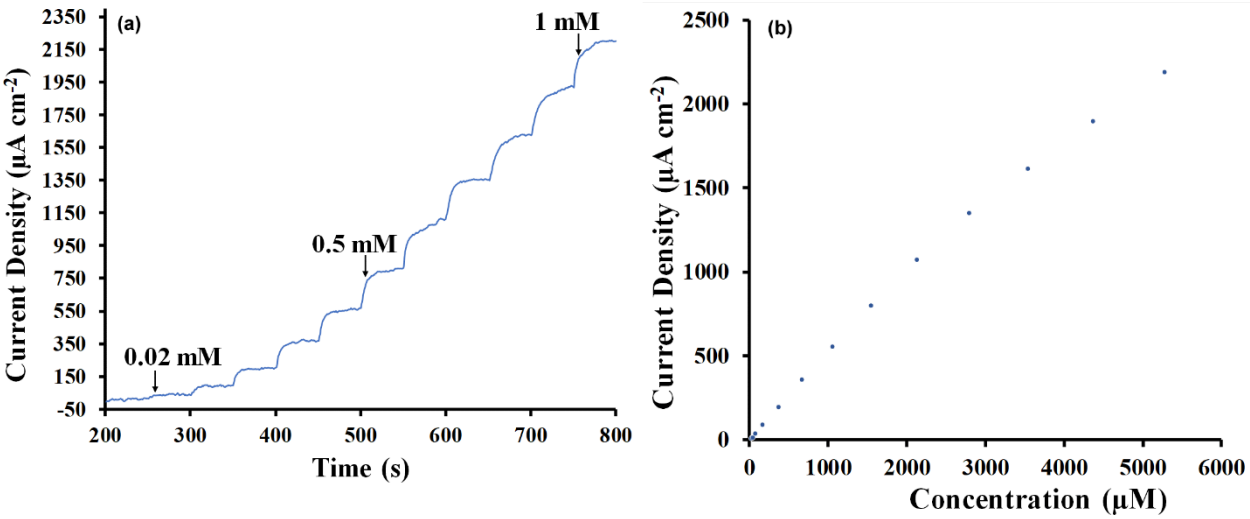

Figure 10. a) Amperometric responses of Pt-N-SPCE upon successive additions of H_2O_2 at different concentrations into 0.05M phosphate buffer (7.4) at -0.4 V. b) Calibration curve for detection of H_2O_2 via amperometry using Pt-N-SPCEs.

Calibration plots (Figure 10b) indicate that the sensor gives a linear response over two distinct ranges. The observation of two linear ranges is attributed to a dominant electrocatalytic mechanism at lower concentrations of H_2O_2, however, direct reduction of H_2O_2 on the surface plays an important role in the analytical signal at higher concentrations of H_2O_2.[57] Good linear relationships between measured current density and H_2O_2 concentration over the ranges of 20 µM to 1.5 mM (R^2=0.9995) (Figure 11a) and 2.1 mM to 5.3 mM (R^2=0.9978) (Figure 11b) were found. Sensitivities of 0.519 (±0.004) µA cm^{-2} $µM^{-1}$ (figure 11a) and 0.353 (0.007) µA cm^{-2} $µM^{-1}$

(Figure 11b) were obtained for the two linear ranges. The linear ranges were determined by removing points in the calibration curve starting from the highest concentration values up to when an acceptable linear regression value was obtained. The sensitivity in the lower concentration range was more than 2-fold higher than that obtained using the N-SPCE. The limit of detection was calculated to be 0.49 µM, which is about 5-fold lower than that found using the N-SPCE.

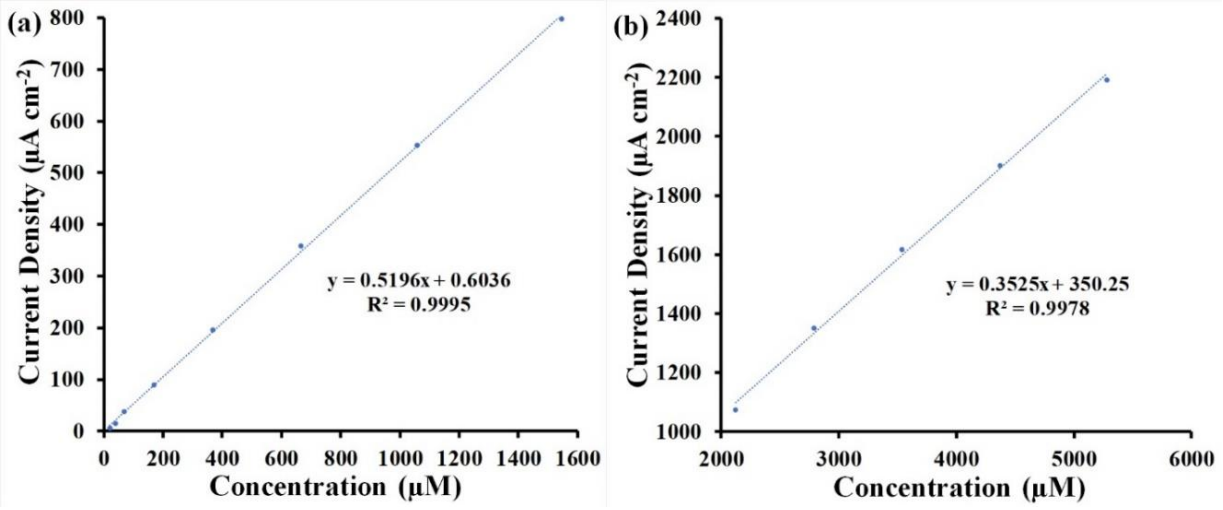

Figure 11. Calibration curves for current density vs H_2O_2 concentration ranging from (a) 20 µM to 1.5 mM and (b) 2.1 mM to 5.3 mM.

The Pt-N-SPCE H_2O_2 sensor compares favorably to other H_2O_2 sensors based on platinum-modified electrodes (Table 4). For example, Niu and coworkers[30] reported a linear range of 5.0 µM to 2.0 mM and limit of detection of 1.23 µM based on screen-printed gold nanofilm electrode modified with platinum nanoparticles decorated carbon nanotubes. Liang and coworkers[56] reported a limit of detection of 0.2 µM using silk composite film electrode modified with spiky platinum nanospheres.

Table 4. Comparison of analytical performance of some platinum-modified amperometric H_2O_2 sensors.

Materials	Linear range (mM)	Sensitivity ($\mu A\ cm^{-2}\ \mu M^{-1}$)	LOD (µM)	Ref.
PtNPs/MWCNT/SPGFE	0.05-2	-	1.23	30
Spiky structured Pt/GS	0-2.5	0.56	0.2	32
PtNPs/graphene paper	0.2-2, 2-8.5	0.06, 0.04	1	57
PtNPs/SPCE	0-0.215	0.69	1.9	58
PtNPs-N-SPCE	0.02-1.5, 2.1-5.3	0.52, 0.35	0.49	This work

CHAPTER 4

CONCLUSION

In conclusion, we fabricated nitrogen-doped screen-printed electrodes using a simple, low-cost and direct method. N-SPCEs were fabricated from graphite that was modified through a simple "soft" nitriding technique using urea. XPS spectra indicated the majority of the nitrogen atoms on the N-carbon (55%) were amine/amide.

The electrocatalytic performance of the fabricated SPCEs, N-SPCEs, and Pt-N-SPCEs were evaluated using cyclic voltammetry and amperometry. The N-SPCEs showed a notable response towards H_2O_2 reduction compared to the bare SPCE. Amperometric responses of SPCEs and N-SPCEs were evaluated using an applied potential of -0.4 V in phosphate buffer solutions. N-SPCE responded to successive addition of different concentrations of H_2O_2 with a characteristic stepwise response where the current increased rapidly to reach a stable value. No change in current on successive addition of the same concentration of H_2O_2 was observed for the SPCE. Calibration plots of current density vs. H_2O_2 concentration indicated a good linear response over the range of 20 μM to 5.3 mM, sensitivity of 0.26 μA cm^{-2} μM^{-1} and a limit of detection of 2.5 μM. The sensor retained 98% of its response after 2 days and 89% after 2 weeks confirming good stability. Reproducibility was also good with average signals from 4 different electrodes differing by no more than 5% over the linear range. The sensor gave a comparable analytical performance towards H_2O_2 reductions to other reported nitrogen-doped electrodes.

PtNP-modified NSPCEs (Pt-NSPCE) were prepared by direct chemical reduction of Pt on N-SPCEs using $NaBH_4$ as the reducing agent [33]. Pt-N-SPCEs showed improved electrocatalytic response towards H_2O_2 reduction compared to N-SPCEs with sensitivities of 0.52 μA cm^{-2} μM^{-1} for H_2O_2 concentrations in the range of 20 μM to 1.5 mM and 0.35 μA cm^{-2}

μM^{-1} for H_2O_2 concentrations in the range of 2.1 mM to 5.3 mM. The limit of detection was 0.49 μM using the Pt-N-SPCE, which is 5-fold better than the N-SPCE.

Overall, N-SPCEs, prepared using simple low-temperature annealing of graphite with urea (two low-cost materials), exhibited good electrocatalytic response and stability towards H_2O_2 reduction. Deposition of PtNPs on N-SPCEs improved electrocatalytic behavior and suggests more versatile applications of N-SPCEs are possible through modification with metal nanoparticles. Further studies will be aimed at demonstrating N-SPCEs as platforms for developing sensors and performing fundamental studies for other electrocatalytic systems that involve N-doped carbons and metal nanoparticles.

REFERENCES

1 Renedo, O. D.; Alonso-Lomillo, M. A.; Martínez, M. J. A. Recent Developments in the Field of Screen-Printed Electrodes and Their Related Applications. *Talanta* **2007**, *73* (2), 202–219.

2 Metters, J. P.; Kadara, R. O.; Banks, C. E. New Directions in Screen Printed Electroanalytical Sensors: An Overview of Recent Developments. *The Analyst* **2011**, *136* (6), 1067.

3 Jewell, E.; Philip, B.; Greenwood, P. Improved Manufacturing Performance of Screen-Printed Carbon Electrodes through Material Formulation. *Biosensors* **2016**, *6* (3), 30.

4 Morrin, A.; Killard, A. J.; Smyth, M. R. Electrochemical Characterization of Commercial and Home-Made Screen-Printed Carbon Electrodes. *Analytical Letters* **2003**, *36* (9), 2021–2039.

5 Wang, J.; Cai, X.; Rivas, G.; Shiraishi, H.; Dontha, N. Nucleic-Acid Immobilization, Recognition and Detection at Chronopotentiometric DNA Chips. *Biosensors and Bioelectronics* **1997**, *12* (7), 587–599.

6 Shih, Y.; Zen, J.-M.; Yang, H.-H. Determination of Codeine in Urine and Drug Formulations Using a Clay-Modified Screen-Printed Carbon Electrode. *Journal of Pharmaceutical and Biomedical Analysis* **2002**, *29* (5), 827–833.

7 Honeychurch, K. C. Screen-Printed Electrochemical Sensors and Biosensors for Monitoring Metal Pollutants. *Insciences Journal* **2012**, 1–51.

8 Hayat, A.; Marty, J. Disposable Screen Printed Electrochemical Sensors: Tools for Environmental Monitoring. *Sensors* **2014**, *14* (6), 10432–10453.

9 Wang, J. Electrochemical Glucose Biosensors. *Chemical Reviews* **2008**, *108* (2), 814–825.

10 Toghill, K. E.; Compton, R. G. Electrochemical Non-Enzymatic Glucose Sensors: A Perspective and an Evaluation. *Int. J. Electrochem. Sci.* **2010**, *5*, 57.

11 Chen, W.; Cai, S.; Ren, Q.-Q.; Wen, W.; Zhao, Y.-D. Recent Advances in Electrochemical Sensing for Hydrogen Peroxide: A Review. *The Analyst* **2012**, *137* (1), 49–58.

12 Hornok, V.; Dékány, I. Synthesis and Stabilization of Prussian Blue Nanoparticles and Application for Sensors. *Journal of Colloid and Interface Science* **2007**, *309* (1), 176–182.

13 Karyakin, A. A. Prussian Blue and Its Analogues: Electrochemistry and Analytical Applications. *Electroanalysis* **2001**, *13* (10), 813–819.

14 Yao, H.; Li, N.; Xu, S.; Xu, J.; Zhu, J.; Chen, H. Electrochemical Study of a New Methylene Blue/Silicon Oxide Nanocomposition Mediator and Its Application for Stable Biosensor of Hydrogen Peroxide. *Biosensors and Bioelectronics* **2005**, *21* (2), 372–377.

15 Shi, Q.; Song, Y.; Zhu, C.; Yang, H.; Du, D.; Lin, Y. Mesoporous Pt Nanotubes as a Novel Sensing Platform for Sensitive Detection of Intracellular Hydrogen Peroxide. *ACS Applied Materials & Interfaces* **2015**, *7* (43), 24288–24295.

16 Niu, X.; Zhao, H.; Chen, C.; Lan, M. Platinum Nanoparticle-Decorated Carbon Nanotube Clusters on Screen-Printed Gold Nanofilm Electrode for Enhanced Electrocatalytic Reduction of Hydrogen Peroxide. *Electrochimica Acta* **2012**, *65*, 97–103.

17 Wang, S. C.; Chang, K. S.; Yuan, C. J. Enhancement of Electrochemical Properties of Screen-Printed Carbon Electrodes by Oxygen Plasma Treatment. *Electrochimica Acta* **2009**, *54* (21), 4937–4943.

18 Shi, L.; Niu, X.; Liu, T.; Zhao, H.; Lan, M. Electrocatalytic Sensing of Hydrogen Peroxide Using a Screen-Printed Carbon Electrode Modified with Nitrogen-Doped Graphene Nanoribbons. *Microchimica Acta* **2015**, *182* (15–16), 2485–2493.

19 Wu, P.; Cai, Z.; Gao, Y.; Zhang, H.; Cai, C. Enhancing the Electrochemical Reduction of Hydrogen Peroxide Based on Nitrogen-Doped Graphene for Measurement of Its Releasing Process from Living Cells. *Chemical Communications* **2011**, *47* (40), 11327.

20 Lyu, Y.-P.; Wu, Y.-S.; Wang, T.-P.; Lee, C.-L.; Chung, M.-Y.; Lo, C.-T. Hydrothermal and Plasma Nitrided Electrospun Carbon Nanofibers for Amperometric Sensing of Hydrogen Peroxide. *Microchimica Acta* **2018**, *185* (8).

21 Karyakin, A.; Karyakina, E.; Gorton, L. Prussian-Blue-Based Amperometric Biosensors in Flow-Injection Analysis. *Talanta* **1996**, *43* (9), 1597–1606. https://doi.org/10.1016/0039-9140(96)01909-1.

22 Ricci, F.; Amine, A.; Palleschi, G.; Moscone, D. Prussian Blue Based Screen-Printed Biosensors with Improved Characteristics of Long-Term Lifetime and PH Stability. *Biosensors and Bioelectronics* **2003**, *18* (2–3), 165–174.

23 Du, D.; Wang, M.; Qin, Y.; Lin, Y. One-Step Electrochemical Deposition of Prussian Blue–Multiwalled Carbon Nanotube Nanocomposite Thin-Film: Preparation, Characterization and Evaluation for H_2O_2 Sensing. *J. Mater. Chem.* **2010**, *20* (8), 1532–1537.

24 Zhang, W.; Wang, L.; Zhang, N.; Wang, G.; Fang, B. Functionalization of Single-Walled Carbon Nanotubes with Cubic Prussian Blue and Its Application for Amperometric Sensing.

25 Hou, Z.; Cai, B.; Liu, H.; Xu, D. Ar, O_2, CHF_3, and SF_6 Plasma Treatments of Screen-Printed Carbon Nanotube Films for Electrode Applications. *Carbon* **2008**, *46* (3), 405–413.

26 Hrapovic, S.; Liu, Y.; Male, K. B.; Luong, J. H. T. Electrochemical Biosensing Platforms Using Platinum Nanoparticles and Carbon Nanotubes. *Analytical Chemistry* **2004**, *76* (4), 1083–1088.

27 Chen, S.; Kucernak, A. Electrodeposition of Platinum on Nanometer-Sized Carbon Electrodes. *The Journal of Physical Chemistry B* **2003**, *107* (33), 8392–8402.

28 Mahajan, A.; Banik, S.; Chowdhury, S. R.; Roy, P. S.; Bhattacharya, S. K. Size Control Synthesis and Amperometric Sensing Activity of Palladium Nanoparticles for Glucose Detection. *Materials Today: Proceedings* **2018**, *5* (1), 2049–2055.

29 Chikae, M.; Idegami, K.; Kerman, K.; Nagatani, N.; Ishikawa, M.; Takamura, Y.; Tamiya, E. Direct Fabrication of Catalytic Metal Nanoparticles onto the Surface of a Screen-Printed Carbon Electrode. *Electrochemistry Communications* **2006**, *8* (8), 1375–1380.

30 Xiangheng N.; Hongli Z.; Chen C.; Minbo L. Platinum Nanoparticle-decorated Carbon Nanotube Clusters on Screen-Printed Gold Nanofilm Electrode for Enhanced Electrocatalytic Reduction of Hydrogen Peroxide. *Electrochimica Acta* **2012**, 65, 97–103.

31 Dhara, K.; Ramachandran, T.; Nair, B. G.; Babu, T. G. S. Fabrication of Highly Sensitive Nonenzymatic Electrochemical H_2O_2 Sensor Based on Pt Nanoparticles Anchored Reduced Graphene Oxide. *Journal of Nanoscience and Nanotechnology* **2018**, *18* (6), 4380–4386.

32 Bo, L.; Lu, F.; Yichuan, H.; Guang, Y.; Qin, Z.; Xuesong, Y. Fabrication and application of flexible graphene silk composite film electrodes decorated with spiky Pt nanospheres. *Nanoscale* **2013**, 00, 1-3.

33 Liu, B.; Yao, H.; Song, W.; Jin, L.; Mosa, I. M.; Rusling, J. F.; Suib, S. L.; He, J. Ligand-Free Noble Metal Nanocluster Catalysts on Carbon Supports via "Soft" Nitriding. *Journal of the American Chemical Society* **2016**, *138* (14), 4718–4721.

34 Cargnello, M.; Chen, C.; Diroll, B. T.; Doan-Nguyen, V. V. T.; Gorte, R. J.; Murray, C. B. Efficient Removal of Organic Ligands from Supported Nanocrystals by Fast Thermal Annealing Enables Catalytic Studies on Well-Defined Active Phases. *Journal of the American Chemical Society* **2015**, *137* (21), 6906–6911.

35 Niu, Z.; Li, Y. Removal and Utilization of Capping Agents in Nanocatalysis. *Chemistry of Materials* **2014**, *26* (1), 72–83.

36 Wang, Y.; Shao, Y.; Matson, D. W.; Li, J.; Lin, Y. Nitrogen-Doped Graphene and Its Application in Electrochemical Biosensing. *ACS Nano* **2010**, *4* (4), 1790–1798.

37 Gong, K.; Du, F.; Xia, Z.; Durstock, M.; Dai, L. Nitrogen-Doped Carbon Nanotube Arrays with High Electrocatalytic Activity for Oxygen Reduction. *Science* **2009**, *323* (5915), 760–764.

38 Maldonado, S.; Stevenson, K. J. Influence of Nitrogen Doping on Oxygen Reduction Electrocatalysis at Carbon Nanofiber Electrodes. *The Journal of Physical Chemistry B* **2005**, *109* (10), 4707–4716.

39 Liu, S.; Yu, B.; Fei, T.; Zhang, T. Low Temperature Thermal Treatment of Hexamethylenetetramine to Synthesize Nitrogen-Doped Carbon for Non-Enzymatic H2O2 Sensing. *Sensors and Actuators B: Chemical* **2014**, *201*, 240–245.

40 Tian, J.; Liu, Q.; Ge, C.; Xing, Z.; Asiri, A. M.; Al-Youbi, A. O.; Sun, X. Ultrathin Graphitic Carbon Nitride Nanosheets: A Low-Cost, Green, and Highly Efficient Electrocatalyst toward the Reduction of Hydrogen Peroxide and Its Glucose Biosensing Application. *Nanoscale* **2013**, *5* (19), 8921.

41 Wu, Y.-S.; Liu, Z.-T.; Wang, T.-P.; Hsu, S.-Y.; Lee, C.-L. A Comparison of Nitrogen-Doped Sonoelectrochemical and Chemical Graphene Nanosheets as Hydrogen Peroxide Sensors. *Ultrasonics Sonochemistry* **2018**, *42*, 659–664.

42 Hummers, W. S.; Offeman, R. E. Preparation of Graphitic Oxide. *Journal of the American Chemical Society* **1958**, *80* (6), 1339–1339.

43 Shuai, H., Yanjin L. Graphene Ink Fabricated Screen-Printed Electrode for Cd^{2+} and Pd^{2+} Determination in Xiangjiang River. *International Journal of Electrochemical Science* **2016**, 7430–7439.

44 Bishop, G. W.; Ahiadu, B. K.; Smith, J. L.; Patterson, J. D. Use of Redox Probes for Characterization of Layer-by-Layer Gold Nanoparticle-Modified Screen-Printed Carbon Electrodes. *Journal of The Electrochemical Society* **2017**, *164* (2), B23–B28.

45 Schneider, C. A.; Rasband, W. S.; Eliceiri, K. W. NIH Image to ImageJ: 25 Years of Image Analysis. *Nature Methods* **2012**, *9* (7), 671–675.

46 Li, X.; Wang, H.; Robinson, J. T.; Sanchez, H.; Diankov, G.; Dai, H. Simultaneous Nitrogen Doping and Reduction of Graphene Oxide. *Journal of the American Chemical Society* **2009**, *131* (43), 15939–15944.

47 Gelius, U.; HedCn, P. F.; Hedman, J.; Lindberg, B. J.; Marine, R.; Nordberg, R.; Nordling, C.; Siegbahn K. Molecular Spectroscopy by Means of ESCA. *Physica Scripta*. **1970**, 2, 70-80.

48 Schaber, P. M.; Colson, J.; Higgins, S.; Thielen, D.; Anspach, B.; Brauer, J. Thermal Decomposition (Pyrolysis) of Urea in an Open Reaction Vessel. *Thermochimica Acta* **2004**, *424* (1–2), 131–142.

49 Randviir, E. P.; Brownson, D. A. C.; Metters, J. P.; Kadara, R. O.; Banks, C. E. The Fabrication, Characterisation and Electrochemical Investigation of Screen-Printed Graphene Electrodes. *Physical Chemistry Chemical Physics* **2014**, *16* (10), 4598.

50 Cumba, L. R.; Foster, C. W.; Brownson, D. A. C.; Smith, J. P.; Iniesta, J.; Thakur, B.; do Carmo, D. R.; Banks, C. E. Can the Mechanical Activation (Polishing) of Screen-Printed Electrodes Enhance Their Electroanalytical Response? *The Analyst* **2016**, *141* (9), 2791–2799.

51 Liu, R.; Li, S.; Yu, X.; Zhang, G.; Zhang, S.; Yao, J.; Keita, B.; Nadjo, L.; Zhi, L. Facile Synthesis of Au-Nanoparticle/Polyoxometalate/Graphene Tricomponent Nanohybrids: An Enzyme-Free Electrochemical Biosensor for Hydrogen Peroxide. *Small* **2012**, *8* (9), 1398–1406.

52 Li, Q.; Mahmood, N.; Zhu, J.; Hou, Y.; Sun, S. Graphene and Its Composites with Nanoparticles for Electrochemical Energy Applications. *Nano Today* **2014**, *9* (5), 668–683.

53 Zhang, Y.; Bo, X.; Nsabimana, A.; Luhana, C.; Wang, G.; Wang, H.; Li, M.; Guo, L. Fabrication of 2D Ordered Mesoporous Carbon Nitride and Its Use as Electrochemical Sensing Platform for H2O2, Nitrobenzene, and NADH Detection. *Biosensors and Bioelectronics* **2014**, *53*, 250–256.

54 Otieno, B. A.; Krause, C. E.; Latus, A.; Chikkaveeraiah, B. V.; Faria, R. C.; Rusling, J. F. On-Line Protein Capture on Magnetic Beads for Ultrasensitive Microfluidic Immunoassays of Cancer Biomarkers. *Biosensors and Bioelectronics* **2014**, *53*, 268–274.

55 Krause, C. E.; Otieno, B. A.; Bishop, G. W.; Phadke, G.; Choquette, L.; Lalla, R. V.; Peterson, D. E.; Rusling, J. F. Ultrasensitive Microfluidic Array for Serum Pro-Inflammatory Cytokines and C-Reactive Protein to Assess Oral Mucositis Risk in Cancer Patients. *Analytical and Bioanalytical Chemistry* **2015**, 407 *(23)*, 7239–7243.

56 Bo L.; Lu F.; Yichuan H.; Guang Y.; Qin Z.; Xuesong Y. Fabrication and Application of Flexible Graphene Silk Composite Film Electrodes Decorated with Spiky Pt Nanospheres. *Nanoscale*, **2013**, 00, 1-3

57 Song, R.-M.; Li, Z.-H.; Wei, P.-J.; Zhao, X.-L.; Chen, C.; Zhu, Z.-G. Flexible Hydrogen Peroxide Sensors Based on Platinum Modified Free-Standing Reduced Graphene Oxide Paper. *Applied Sciences* **2018**, *8* (6), 848.

58 Agrisuelas, J.; González-Sánchez, M.-I.; Valero, E. Hydrogen Peroxide Sensor Based on in Situ Grown Pt Nanoparticles from Waste Screen-Printed Electrodes. *Sensors and Actuators B: Chemical* **2017**, *249*, 499–505.

VITA

CHIDIEBERE OGBU

Education:

MS Chemistry, East Tennessee State University, Johnson City, TN, 2019.

B.Eng. Polymer & Textile Engineering, Federal University of Technology Owerri, Nigeria, 2013.

Professional Experience:

Field Service Engineer, Poseidon Energy Services, Port Harcourt, Nigeria, (2013 - 2017).

Graduate Teaching Assistant, East Tennessee State University, Johnson City TN, (2017 – 2019).

Research Assistant, (Dr. Gregory Bishop's Research Lab), East Tennessee State University, Johnson City, TN (2019).

Research Experience:

Graduate research student, East Tennessee State University, Johnson City TN (2017 -2019)
(Mentor: Dr. Gregory Bishop)

Fabricated 3D-printed fluidic devices for biosensing applications.

Fabricated nitrogen doped screen-printed electrodes and determined their electrocatalytic activity.

Conducted electrochemical measurements.

Presentations:

Elisha Adeniji, Chidiebere Ogbu, and Gregory W. Bishop
"Peroxide Sensing and Gold Nanoparticle Deposition using Nitrogen-Doped Screen-Printed Electrodes"
2018 Eastman-NETSACS Student Research symposium
(10/16/2018, Poster Presentation, Eastman-NETSACS 2019)

Chidiebere Ogbu and Gregory W. Bishop.
“Peroxide Sensing using Nitrogen Doped Screen-Printed Carbon Electrodes”, 2019 Appalachian Student Research Forum, East Tennessee State University, Johnson City TN.
(04/12/2019, Oral Presentation, ASRF 2019).

Chidiebere Ogbu and Gregory W. Bishop.
“Peroxide Sensing Using Nitrogen-Doped Screen-Printed Carbon Electrodes”. Graduate Seminar, East Tennessee State University, Johnson City, TN
(5/24/2019, Oral Presentation)